Coverage dependent desorption dynamics of deuterium on Si(100) surfaces: Interpretation with a diffusion-promoted desorption model

doi: 10.1063/1.1829994

Coverage dependent desorption dynamics of deuterium on Si(100) surfaces: Interpretation with a diffusion-promoted desorption model

T. Matsuno, T. Niida, H. Tsurumaki, and A. Namiki[a)]
Department of Electrical Engineering, Kyushu Institute of Technology, Kitakyushu 804-8550, Japan

(Received 9 July 2004; accepted 18 October 2004; published online 17 December 2004)

We studied coverage dependence of time-of-flight (TOF) spectra of D_2 molecules thermally desorbed from the D/Si(100) surface. The mean translational energies $\langle E_t \rangle$ of desorbed D_2 molecules were found to increase from 0.20 ± 0.05 eV to 0.40 ± 0.04 eV as the desorption coverage window was decreased from $1.0\,\mathrm{ML} \geqslant \theta_D \geqslant 0.9\,\mathrm{ML}$ to $0.2\,\mathrm{ML} \geqslant \theta_D \geqslant 0\,\mathrm{ML}$, being consistent with the kinetics switch predicted in the interdimer mechanism. The measured TOF spectra were deconvoluted into 2H, 3H, and 4H components by a curve fitting method along the principle of detailed balance. As a result, it turned out that the desorption kinetics changes from the 4H to the 3H situation at high coverage above $\theta_D = 0.9\,\mathrm{ML}$, while the 2H desorption is dominant for a quite wide coverage region up to $\theta_D = 0.8\,\mathrm{ML}$. A dynamic desorption mechanism by which the desorption is promoted by D-atom diffusion to dangling bonds was proposed. © *2005 American Institute of Physics.* [DOI: 10.1063/1.1829994]

I. INTRODUCTION

The adsorption/desorption of hydrogen on the Si surfaces is a prototype of gas-covalent solid surface interaction. The principle of detailed balance is of paramount significance in understanding reaction dynamics of hydrogen on the surfaces.[1,2] In the last decade, however, the adsorption/desorption dynamics of hydrogen on the Si(100) surface has been a subject of theoretical controversy because of an apparent violation of detailed balance: In spite of the high adsorption barrier no translational heating was observed in pulsed-laser-desorption (PLD).[3] Contrary to this result, however, the recent experiments on adsorption[4,5] and desorption[6,7] have supported the general validity of detailed balance. This is because a considerable translational heating was recognized in the time-of-flight (TOF) spectra measured under the equilibrium condition of conventional temperature-programmed desorption (TPD). The discrepancy, which appeared in the PLD and TPD studies, may be partly due to the methods employed and partly due to the hydrogen coverage studied.

To date, the interdimer mechanism has been strongly supported in the experimental[8–12] and theoretical[13–16] studies. The interdimer mechanism includes three possible situations, the 4H, 3H, and 2H situation, depending on the number of H atoms relevant to the reaction sites at one end of a pair of adjacent Si dimers on which the adsorption or desorption reaction takes place. It has been experimentally suggested that adsorption along the 4H pathway is barrierless[8–10] while that along the 2H or 3H pathway is activated by incident energy E overcoming the adsorption barrier $\geqslant 0.6$ eV or ~ 0.2 eV, respectively.[10] The site specific sticking coefficients s are more than two orders of magnitude smaller for the 3H channel desorption than for the 4H one.[10] In view of detailed balance, as the hydrogen coverage is decreased in TPD on a fully saturated one mono layer (ML) surface, the desorption kinetics is expected to switch from the 4H to 2H situation, presumably with a negligible contribution by the 3H one. The desorption dynamics is then anticipated to also switch concomitantly to this kinetics switch. The 4H/2H crossover coverage θ_{cross} in TPD was studied by Zimmermann and Pan for the first time.[9] They predicted that $\theta_{cross} \simeq 0.1\,\mathrm{ML}$. However, this was not supported by the TOF experiments since the translational heating was observed to occur for a quite wide coverage region up to 0.8 ML.[6,7] On the other hand, employing nonequilibrium thermodynamics theory, Brenig, Kreuzer, and Payne predicted that $\theta_{cross} = 0.5-0.7\,\mathrm{ML}$, above which neither translational nor vibrational heating were anticipated.[16]

In the previous TOF studies,[6,7] desorption events occurring at high coverages above 0.8 ML and also at low coverages below 0.1 ML were intentionally discarded to detour contaminant desorptions arising from dihydrides and subsurface hydrogens, respectively. As outlined above, for understanding the mechanism of hydrogen desorption from the Si(100) surface information on desorption dynamics particularly at higher coverages around 1.0 ML is strongly required. In this paper we report dependence of mean translational energies $\langle E_t \rangle$ on D coverage for D_2 molecules desorbed from the Si(100) surface. We find a somewhat abrupt increase in $\langle E_t \rangle$ from approximately 0.2 to 0.4 eV with decreasing desorption coverage from 1.0 to 0.5 ML. This fact suggests an occurrence of kinetics switch from the 4H to 2H situation, probably via the 3H one.

II. EXPERIMENT

TOF spectra of D_2 molecules desorbed along the surface normal from the Si(100) surface were measured by means of a cross-correlation method as described previously.[6] In order to measure coverage dependent TOF spectra, data were collected for molecules desorbed during either of a whole or of

[a)]Electronic mail: namiki@ele.kyutech.ac.jp

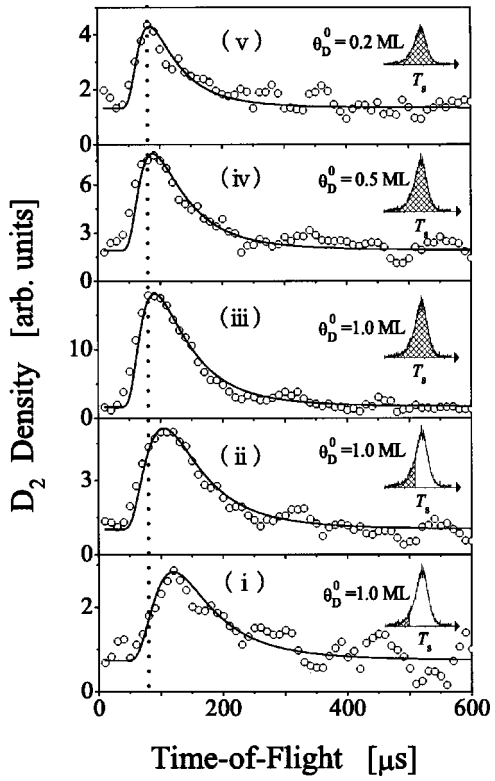

FIG. 1. TOF density spectra of D_2 molecules desorbed from the D/Si(100) surface for various desorption coverage windows. TOF data were collected for the coverage windows (i) 1.0–0.9, (ii) 1.0–0.75, (iii) 1.0–0.0, (iv) 0.5–0.0, and (v) 0.2–0.0 ML, along the hatched area of TPD spectra in the insets. The solid lines show the smoothed curves obtained after fitting to Eq. (1) in the text with three nonshifted Maxwellian functions characterized with translational temperatures of 2500, 1500, and 800 K.

a selected leading edge of β_1 channel TPD spectra with various initial coverages θ_D^0. Generally, a hundred TPD spectral scans were repeated for one TOF spectrum. In order to know coverage dependence of TOF spectra we chose five coverage conditions: (i) 1.0–0.9, (ii) 1.0–0.75, (iii) 1.0–0.0, (iv) 0.5–0.0, and (v) 0.2–0.0 ML, where the first and the second values stand for the initial (also θ_D^0) and final coverage, respectively. The widths of the coverage windows employed were thus different among the five TOF spectra. Saturated 1.0 ML D/Si(100) surfaces were prepared with a special care so that no dideuterides were formed under the condition of surface temperature of 573 K during D irradiation. The subsurface deuterium atoms were minimized by preparing the well annealed surfaces for the minimum D irradiation time. Data collections with a multichannel scaler were manually gated for the controlled coverage windows by monitoring each TPD spectral trace (6 K/s heating rate) on a scope of a quadrupole mass spectrometer.

III. RESULTS

Figure 1 shows five TOF spectra obtained under the above defined coverage conditions. It is clearly observed that the peak of the TOF curves for the high coverage regime (i) and (ii) is located at much later time region than the case of the low coverage regime (v) or (iv). This implies that $\langle E_t \rangle$ is considerably decreased for the coverage region only above

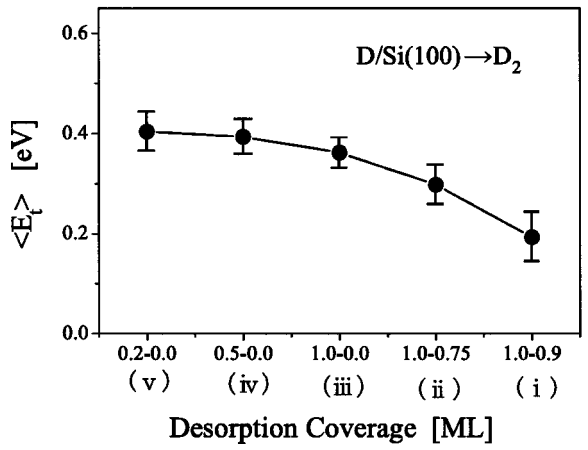

FIG. 2. Plots of mean translational energies $\langle E_t \rangle$ of D_2 molecules desorbed from the Si(100) surfaces for the five coverage windows. The solid lines are the guide for eyes.

0.75 ML, suggesting desorption kinetics switches at high coverage above 0.75 ML from a high to low barrier pathway. The TOF curve for (iii) which covers the whole desorptions from 1 to 0 ML shows up no such a clear delay in the peak position, compared to those observed for (v) or (iv). This fact indicates that the main desorptions from the 1.0 ML saturated surface can be attributed to such desorptions that proceeded overcoming the high adsorption barriers similar to (v) or (iv).

The measured raw TOF data exhibits density rather than flux. To evaluate $\langle E_t \rangle$ the TOF density data are first corrected to flux data by multiplying $1/t$. Because of small desorption yields, S/N ratios of the measured TOF spectra for (i) and (v) are a bit poor. Large fluctuation, which appeared in a faster time region, is amplified when the density data are changed to flux one. This results in an ambiguity in evaluating $\langle E_t \rangle$. To avoid this problem, the raw TOF data were first smoothed by fitting to a linear combination of nonshifted Maxwellians (density) characterized with translational temperatures T_j,

$$f(t) = \sum_j c_j t^{-4} \exp\{-mL^2/2t^2 k T_j\}, \tag{1}$$

where c_j is the intensity of the jth component, m is the mass of a D_2 molecule, and L is the 33.2 cm long flight distance. It turned out that once T_j's are fixed as common temperatures for the five TOF spectra, reasonable curve fit requires at least three Maxwellians, $j=1$, 2, and 3. Allowing ± 100 K ambiguities we determined $T_1=2500$, $T_2=1500$, and $T_3=800$ K. Adjusting three intensities, c_1, c_2, and c_3, for the corresponding three Maxwellian functions, we obtained smoothed curves of the raw TOF curves. Solid lines in Fig. 1 are the so obtained smoothed curves. We evaluated $\langle E_t \rangle$ from these smoothed curves by

$$\langle E_t \rangle = \frac{\int_0^\infty \frac{1}{2t} m \left(\frac{L}{t}\right)^2 f(t)\,dt}{\int_0^\infty \frac{1}{t} f(t)\,dt}.$$

Results for the five coverage windows are plotted in Fig. 2.

With increasing coverage from (v) to (i), $\langle E_t \rangle$ decreases from 0.40 ± 0.04 eV to 0.20 ± 0.05 eV. For $\theta_D \leqslant 0.5$ ML, $\langle E_t \rangle$ remains mostly unchanged, but it rapidly decreases for $\theta_D \geqslant 0.75$ ML. Notice that the value of $\langle E_t \rangle = 0.20$ eV for the high coverage (i) is agreeable with that obtained in PLD.[3]

IV. DISCUSSION

A. Applying detailed balance: The 2H/3H/4H interdimer mechanism

Such a large shift in $\langle E_t \rangle$ with coverages as shown in Fig. 2 may not be explained with any types of single dynamics mechanism such as the intradimer[17] or the isolated dihydride[18] desorption mechanism even if it is allowed to include the $v=1$ vibrational excitation [$\simeq 8\%$ (Ref. 19)]. The TOF spectrum comprises more than two components depending on the coverage or various D/Si configurations. We recognize that for $\theta_D \simeq 1.0$ ML, the molecules have passed a transition state without any noticeable adsorption barriers since $\langle E_t \rangle$ tends to $2kT_s$ ($=0.13$ eV at 780 K). On the other hand, for $\theta_D \leqslant 0.5$ ML they have overcome appreciably high adsorption barriers. Thus the TPD kinetics on the 1.0 ML D-terminated surface must switch from a barrierless pathway to a different pathway with a nonzero energy barrier. The crossover between the two desorption situations with and without barriers may occur above 0.75 ML since it is found that $\langle E_t \rangle$ abruptly decreases there. Since the observed feature has been theoretically predicted along the 2H/4H interdimer mechanism,[16] this change in the desorption dynamics seems not to be at variance with the interdimer mechanism.

We therefore analyze the TOF spectra along the interdimer mechanism with the 2H and 4H as well as with 3H pathway. Detailed balance is the principle that relates desorption and adsorption dynamics via a sticking coefficient s. In order to get TOF functions to fit to the data, we rely on this principle on the basis of the recent adsorption[4,10] and desorption[6,7] experiments. A desorption flux function $f(E)$ is expressed as a sum of three components, f_{2H}, f_{3H}, and f_{4H}, for the 2H, 3H, and 4H desorption pathways,

$$f(E)(=f_{2H}+f_{3H}+f_{4H}) = E\exp(-E/kT_s)\{c_{2H}s_{2H}(E,T_s)+c_{3H}s_{3H}(E,T_s) + c_{4H}s_{4H}(E,T_s)\}. \quad (2)$$

Here, c_i stands for the intensity for $i=2$H, 3H, or 4H desorption component. For the 2H and 3H pathways, $s_i(E,T_s)$ has been empirically expressed with a sigmoid curve as a function of $\tanh(x)$ where x includes both the threshold energy $E_{0,i}$ and the width parameter W_i,[4,10]

$$s_i(E,T_s) = \frac{A_{0,i}}{2}\left\{1+\tanh\left(\frac{E-E_{0,i}}{W_i(T_s)}\right)\right\}, \quad (3)$$

where $A_{0,i}$ is the saturated sticking coefficient at $E=+\infty$ for the 2H or 3H pathway. Since s_{4H} decreases with E,[10] it can be expressed as a reversed sigmoid curve,

$$s_{4H}(E) = \frac{A_{0,4H}}{2}\left\{1-\tanh\left(\frac{E+E_{0,4H}}{W_{4H}(T_s)}\right)\right\}. \quad (4)$$

Here, $A_{0,4H}$ is the saturated sticking coefficient at $E=-\infty$. For such a barrierless adsorption pathway, $E_{0,4H}$ is allowed to be negative.

In order to analyze the measured TOF spectra along the principle of detailed balance, the energy flux function, Eq. (2), should be changed to a TOF density distribution function,

$$f(t) = \sum_{j=2H,3H,4H} c_j t^{-4}\exp\{-m(L/t)^2/2kT_s\} \times s_j(E=m(L/t)^2/2,T_s). \quad (5)$$

Detailed balance is the principle that is valid for adsorption and desorption occurring under the same equilibrium conditions. Regarding this point, T_s is an important variable on which the parameters in Eqs. (3) and (4) depend. Particularly, W is an increasing function of T_s as found for the low coverage case[4] or for the 2H process. The surface temperatures employed in the adsorption experiments (<700 K) are usually quite lower than in the desorption experiments ($\geqslant 700$ K). Besides, the beam experiments were done for hydrogen but not deuterium. Some isotope effects could be present in adsorption/desorption reactions. At present, therefore, the parameters for s determined in the H_2 adsorption experiments may not be straightforwardly applied to the D_2 desorption studies. While the previously reported values[4,6,10] are taken into account, we may need to appropriately adjust $E_{0,i}$ and W_i so that $f_i(E)$ can become closer to each of the three nonshifted Maxwellians used before to smooth the raw TOF data. This approach may be reasonable at least for both the 2H and 4H situations. This is because if $(E_0-E)/W > 1.0$ and $W \geqslant 3kT_s$, $f(E)[=E\exp(-E/kT_s)s(E,T_s)]$ can be approximated with a nonshifted Maxwellian characterized with a heated translational temperature $T_t \simeq [W/(W-2kT_s)]T_s$.[6,7] As was obtained previously[6,7] and will be evaluated below, the desorption in the low coverage regime, thus along the 2H pathway, is characterized with $W_{2H} \sim 3kT_s$ ($\simeq 0.2$ eV for $T_s=780$ K). This yields $T_t=3T_s$ (~ 2340 K), which is very close to $T_1(=2500$ K) as evaluated for Eq. (1). For the 4H desorption that occurs exclusively on the 1 ML saturated surface, such a nonshifted Maxwellian characterized with $T_t \simeq T_s$ is much more straightforwardly derived from the term $f_{4H}(E)=c_{4H}E \times \exp(-E/kT_s)s_{4H}(E,T_s)$ since $s_{4H}(E,T_s)$ is nearly constant for $E \leqslant 0.35$ eV.[10] We can therefore predict that $f_{4H}(E) \propto E\exp(-E/kT_s)$. In this way, for the high coverage regime the Maxwellian characterized with $T_3=800$ K± 100 K in Eq. (1) can be unambiguously attributed to desorption along the 4H pathway. This may justify the nonheated translations observed in the PLD experiments[3] provided that they were done at a high coverage regime around 1.0 ML.

For the 3H situation, however, neither a condition $(E_{0,3H}-E)/W_{3H}>1$ nor condition such that sticking coefficient is nearly constant may be fulfilled for $E \leqslant 0.3$ eV, since $E_{0,3H}$ is not large compared to $E_{0,2H}$.[10,14] Therefore, f_{3H} is no longer approximated simply with a nonshifted Maxwellian characterized with a certain translational temperature. This implies that the nonshifted Maxwellian determined as the second component ($T_2=1500$ K) in Eq. (1) cannot be

straightforwardly referenced in obtaining the parameters $E_{0,3H}$ and W_{3H}. [This is the reason why we do not discuss the deconvolution results of the TOF curve along Eq. (1) for the 2H/3H/4H interdimer mechanism.]

On the basis of the above mentioned considerations, we now determine the values of parameters for each sticking coefficient from a desorption point of view. Taking actual desorption temperatures at representative portions of TPD spectra into account, average desorption temperatures of 710, 740, and 780 K are taken at the leading edge, at around the maximum slope, and at the maximum of the peak, respectively. For the 2H situation, we choose $E_{0,2H}=1.0$ eV, $W_{2H}(780\,\mathrm{K})=0.195$ eV, and $W_{2H}(740\,\mathrm{K})=0.18$ eV. The value of 1.0 eV for $E_{0,2H}$ is the upper limit of the reported value.[4] For these parameters, we obtain $\langle E_t\rangle_{2H}=0.38$ eV or $T_{2H}(=\langle E_t\rangle/2k)=2280$ K. The latter value is close to T_1 $(=2500\pm100\,\mathrm{K})$ evaluated after fitting with Eq. (1). For the 3H situation we take $E_{0,3H}=0.30$ eV and $W_{3H}(710\,\mathrm{K})=0.17$ eV, which are compared with the adsorption data $E_{0,3H}=0.19\pm0.03$ eV and $W_{3H}(350\,\mathrm{K})=0.076$ eV.[10] The large difference in W_{3H} found between the adsorption and desorption data may be due to influence of T_s. We calculate the mean translational energy for the 3H pathway $\langle E_t\rangle_{3H}=0.21$ eV or $T_{3H}(=\langle E_t\rangle_{3H}/2k)=1260$ K, which is about 20% smaller than $T_2(=1500\pm100\,\mathrm{K})$ evaluated in Eq. (1). For the 4H pathway for which $s_{4H}(E)$ is decreased with E, the values of $E_{0,4H}$ and W_{4H} in Eq. (4) were not determined in the beam experiments.[10] Apart from $A_{0,4H}$, we try to determine them in such a way that relative line shape of Eq. (4) can be best fit to $s_{4H}(E)$ obtained in the beam experiment. As a result, we find $E_{0,4H}$ and $W_{4H}(710\,\mathrm{K})$ are not uniquely determined because the measured $s_{4H}(E)$ curve is more or less flat. Therefore, the finally employed values, $E_{0,4H}=-0.20$ eV and $W_{4H}(710\,\mathrm{K})=0.30$ eV, are still tentative. Nevertheless, this ambiguity does not seriously alter the result on the desorption dynamics since s_{4H} is insensitive to the two parameters. Consequently, extent of translational cooling, which is a general trend in desorptions arising from systems characterized with such barrierless adsorptions, is found to be small for the wide range of variations of the two parameters, namely, $\langle E_t\rangle_{4H}\simeq0.12$ eV or $T_{4H}(=\langle E_t\rangle_{4H}/2k)\simeq710$ K.

The raw TOF spectra are fitted with Eq. (5) with the three TOF functions defined above by adjusting their intensities. In the actual practice of fitting, since the saturated sticking constants $A_{0,i}$ cannot be determined in the present desorption experiments they are included into c_i. In Fig. 3 we plot the fit results over the five raw TOF spectra. For the low coverage case (iv) or (v), it is obvious that the TOF spectrum mainly comprises desorptions along the 2H pathway. The spectrum also comprises a small (~8%) component in the later TOF region. Since the 2H pathway accompanies vibrational excitation of the molecules[16] which was indeed observed in the laser spectroscopic studies,[19] this small component could be attributed to the $v=1$ vibrationally excited molecules overcoming high barriers rather than to the barrierless 4H desorption. According to the principle of detailed balance, one can expect that translational energies of such vibrationally excited hydrogen molecules

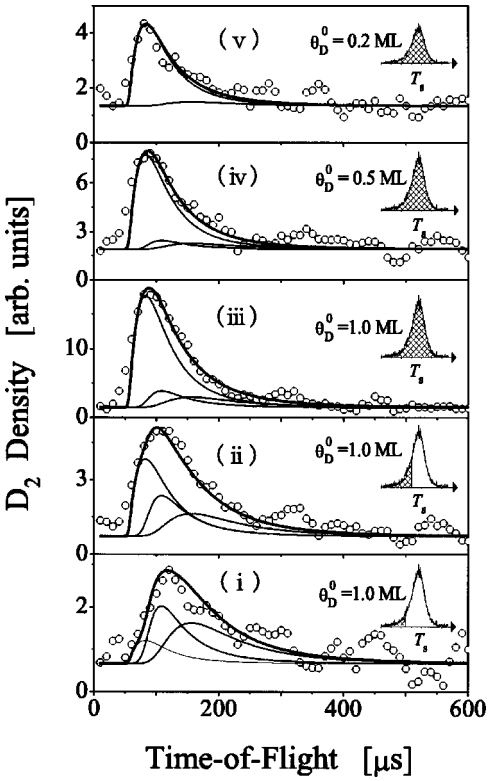

FIG. 3. Fits of TOF curves with the desorption function, Eq. (5), in the text. The open circles are the experimental data same to those in Fig. 1. The three thin solid lines in each panel are the components of f_{2H}, f_{3H}, and f_{4H} in the order of the peak positions from the fast to slow time region, respectively. The thick solid lines are the sum of the three components.

desorbing from surfaces are characterized with lower translational energies than that of the vibrationally nonexcited molecules since they can stick to the surface with lower energies than that of the ground state molecules.[4] For the high coverage cases (i) and (ii), on the other hand, the 4H (and 3H) component increases in intensity while the 2H component decreases with coverage. This anticorrelation between the 2H and 4H components indicates that the net increase of the 4H component at the high coverage regime is attributed to desorption not along the 2H pathway but along the 4H one.

After correcting the density data to flux one, the fraction of each component in the TOF spectra is evaluated. Results are plotted in Fig. 4 for the five TOF spectra. While the 2H component decreases with coverage, both the 3H and 4H components concomitantly increase. Taking both of the wider coverage windows employed and the possible inclusion of the $v=1$ molecules in the 2H pathway into account, it should be noticed that the 2H component crosses with the 3H and 4H one at the coverage region around 0.8 ML. For (i), the highest desorption coverage used in this study, the 3H and 4H situations are found to equally share the desorption. This fact suggests that the desorption along the 4H pathway becomes dominant only at the very high coverage region for $\theta_D\geqslant0.9$ ML. Dürr *et al.*[12] observed the preferential 4H desorption in the STM experiments combined with PLD at a very narrow coverage window around 1.0 ML.

For the desorption coverage window 1.0–0.0 ML in Fig.

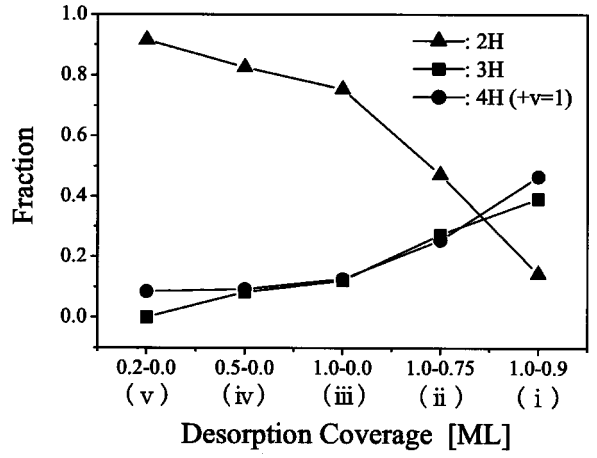

FIG. 4. Plots of fraction of the 2H, 3H, and 4H (including vibrationally excited $v=1$ component) components for the five coverage windows (i), (ii), (iii), (iv), and (v). The solid lines are the guide for eyes.

3 (iii), the net 1.0 ML desorption comprises a superposition of desorptions along the 4H, 3H, and then 2H pathway, each of which is dependent on the momentary surface coverage during TPD. Considering the possible inclusion of $v=1$ vibrationally excited molecules in the 4H component into account, 8% of the 2H desorption flux is subtracted from the 4H desorption flux, and then it is added to the 2H desorption flux. As a result, fractions of the 2H, 3H, and 4H desorption flux are evaluated to be $81\pm8\%$, $12\pm3\%$, and $7\pm3\%$, respectively. We therefore conclude that the 2H pathway is the predominant desorption channel over the 4H and 3H pathways for a quite wide coverage range from zero to 0.8 ML. This means once a fraction of D adatoms were inevitably lost at the leading edge in TPD spectral scans, the kinetics and dynamics of hydrogen desorptions studied over the main temperature region of the TPD spectrum are solely attributed to the desorption along the 2H pathway.

The reaction dynamics of hydrogen on the Si surfaces may be characterized not only with translational and vibrational degrees of freedom of molecules but also with vibrational degrees of freedom of substrate Si atoms. Detailed balance is valid provided that dynamics of Si atoms during reaction is also taken into account. The sigmoid curve, Eq. (3), implicitly includes effect of lattice dynamics through W which is a function of T_s. For the adsorption along the 2H pathway, activation energy E_{Arr} as defined in an Arrhenius type sticking rate constant is a function of incident energy E. E_{Arr} has been analytically, but approximately, given as[6]

$$E_{\mathrm{Arr}}(E)=\frac{2kT_s}{W_{2\mathrm{H}}(T_s)}(E_{0,2\mathrm{H}}-E). \tag{6}$$

Equation (6) allows one to know a relationship between the energy of the adsorption barrier for the 2H pathway ($E_{\mathrm{ad,2H}}$) and the threshold energy ($E_{0,2\mathrm{H}}$) defined in Eq. (3). Generally, adsorption energy barrier is determined from E_{Arr} for $E=0$, i.e., $E_{\mathrm{ad,2H}}=E_{\mathrm{Arr}}(E=0)$. Thus, it does not necessarily mean that $E_{0,2\mathrm{H}}=E_{\mathrm{ad,2H}}$. Taking the typical values for the parameters, i.e., $E_{0,2\mathrm{H}}=1.0\,\mathrm{eV}$ and $W_{2\mathrm{H}}(T_s)=3kT_s$, we evaluate $E_{\mathrm{ad,2H}}[=E_{\mathrm{Arr}}(E=0)]=0.66\,\mathrm{eV}$, which is very close to the value of 0.68 eV or 0.63 ± 0.09 eV evaluated in the desorption rate data analysis[9,16] or in a quantum Monte Carlo theory,[15] respectively.

Applying detailed balance to Eq. (6), one can estimate the energy release to the Si lattice after desorption. Since desorption is the reversed process of adsorption, desorbing molecules with translational energy E have left behind E_{Arr} on the surface, exciting Si lattice vibrations or phonons. After taking the same parameter values as used above and $E=0.4\,\mathrm{eV}$, one may get $E_{\mathrm{Arr}}=0.4\,\mathrm{eV}$. Thus, the threshold energy $E_{0,2\mathrm{H}}$ is disposed equally to both the translational degree of freedom of molecules and the vibrational degree of freedom of substrate Si atoms, and partly to the internal degrees of freedom of the molecules as well.

B. Diffusion-promoted desorption model

It is very surprising to see that the desorption along the 4H pathway is inefficient even at high coverages around 0.8 ML where the 4H configuration, i.e., a pair of adjacent doubly occupied Si dimers, is predominant. Such predominance of 4H configuration is also the case even in the lower coverage region around 0.5 ML, since the recent STM experiment reveals that a 0.5 ML H/Si(100) surface prepared at 700 K, where thermal desorption takes place, has a surface structure patched with H-terminated regions.[20] In spite of repulsive interaction among doubly occupied Si dimers, attractive interaction between bare Si dimers gets rid of doubly occupied Si dimers to form occupied Si-dimer clusters.[20] The distribution of the cluster size has a maximum at around four Si dimers extending to more than 10 Si dimers. Similar results were also reported recently.[21,22] On the other hand, for $E\leqslant0.2\,\mathrm{eV}$ where the Maxwell-Boltzmann flux $E\exp(-E/kT_a)$ becomes large with its maximum at around $E\simeq0.07\,\mathrm{eV}$ for $T_s=780\,\mathrm{K}$, one knows that $s_{4\mathrm{H}}>10^{-4}$ while $s_{2\mathrm{H}}<10^{-7}$ (Refs. 4 and 10). Considering that desorption rate is proportional to a product of s and density of the relevant desorption configuration, the observed predominance of the 2H desorption over the 4H one is therefore quite unexpected.

In the framework of the 2H/4H nonequilibrium thermodynamics Brenig *et al.*[16] succeeded to predict a high 2H/4H crossover coverage around 0.5 ML, which is however still lower than the present result. They found that it can be further increased by only small changes in the interaction parameters to control the distribution of hydrogen configurations relevant to each desorption pathway. However, they noticed that changing the parameter values accompanies a deviation of the calculated s from the experimental one.[9] The 2H/4H interdimer mechanism may not properly explain the experimentally established first-order desorption kinetics since the apparent desorption order is determined from the subtle intensity balance between the 2H and 4H desorption rates. Indeed, we can derive a nearly 1.3rd-order desorption kinetics from the rate versus coverage curve for $T_s=776\,\mathrm{K}$ plotted in Fig. 2 of Ref. 16. The 2H/4H interdimer mechanism neglects the contribution of the 3H pathway because of too small $s_{3\mathrm{H}}$ compared with $s_{4\mathrm{H}}$. However, we recognize that it is not negligible for $\theta_{\mathrm{D}}\sim0.9\,\mathrm{ML}$ in this work.

In addition to these unsolved problems, there is another problem to be seriously considered for the desorption kinet-

ics: Recently, Filippi *et al.*[15] calculated the energetics relevant to the 2H and 4H reaction pathways on the basis of the quantum Monte Carlo calculation, presently one of the best reliable theoretical methods. As a result, the desorption and adsorption energy barriers were evaluated to be $E_{\mathrm{des,2H}}=2.91\pm0.09$ eV and $E_{\mathrm{ad,2H}}=0.63\pm0.09$ eV for the 2H pathway, and $E_{\mathrm{des,4H}}=2.84\pm0.12$ eV and $E_{\mathrm{ad,4H}}=0.19\pm0.14$ eV for the 4H pathway. The result $E_{\mathrm{ad,2H}}=0.63\pm0.09$ eV agrees well with the experimental results $E_{\mathrm{ad,2H}}\simeq0.65$ eV as noted in the preceding section. This should be compared to the result $E_{\mathrm{ad,2H}}=0.2$ eV obtained using a PW91 functional with a GGA correction,[14] by which the adsorption as well as desorption barriers are thus seriously underestimated. For the desorption processes, the quantum Monte Carlo theory slightly prefers the 4H pathway to the 2H one. However, within error bars the difference between the two desorption barriers is small regardless of whether the adsorption barrier is very high along the 2H pathway or quite low along the 4H one. More importantly noticed is the fact that the calculated desorption barriers are considerably higher than the experimentally established value of $\sim$2.5 eV.[23] They explained this discrepancy by stating that desorption in experiments occurs at steps or defect sites where the desorption barrier is lowered. However, this explanation seems to apparently contradict the applicability of detailed balance found in the dynamic desorption and adsorption experiments. Namely, sticking to D_B steps occurs overcoming as low as 0.1 eV barriers,[10] which suggests that $\langle E_t\rangle$ would be remarkably lower than that along the 2H pathway. However, this is not the case in desorption as noticed in this work. We consider some physics other than the influence of steps or surface defects must be involved behind.

In order to reconcile the discrepancies hitherto found in the theories and experiments as noted above, i.e., first-order desorption kinetics, inefficacy of the 4H desorption pathway compared to the 2H and 3H pathways, and substantial decrease of the desorption energy barriers in actual experiments, we propose a diffusion-promoted desorption mechanism. As was found in this work, desorption along the 4H pathway is really restricted on the nearly saturated surface, but once the dangling bonds are created it is easily replaced by the 3H or 2H one. This suggests that the presence of dangling bonds plays a key role in desorption. The proposed mechanism is based on an idea that the desorption along the 2H or 3H pathway is promoted by diffusion (hopping) of H(D) adatoms to dangling bonds, whereas the 4H pathway is not promoted since saturated surfaces do not allow H(D)-atom diffusion. It is well known that at higher temperatures above 700 K, where desorption actually occurs, H adatoms efficiently diffuse to dangling bonds along but not across Si dimer rows.[24,25] The diffusion barrier along Si dimer rows has been evaluated to be about 1.6 eV,[24,25] which is much lower than the desorption barrier. For $T_s\sim800$ K, the rate of H-atom diffusion to nearby dangling bonds ($\sim10^5\,\mathrm{s}^{-1}$) is orders of magnitude higher than the typical TPD rate ($\leqslant10^{-1}\,\mathrm{s}^{-1}$).[24,25] This means the dangling bonds that will take part in the 2H or 3H situation receive more than 10^6 times of H-atom diffusions prior to desorption.

In addition to the STM experiments,[24] deuterium desorptions affected by oxygen adatoms may also give experimental evidence of such adatom diffusion prior to TPD: Tsurumaki *et al.*[26] found that 0.1 ML oxygen atoms on Si(100) surfaces tend to inhibit D atoms to stick to O-adsorbed sites. However, deuterium desorptions for a low coverage regime below 0.1 ML was found to occur preferentially from such O-adsorbed sites where desorbed D_2 molecules exhibit a TPD peak around 1000 K. This observation strongly suggests that D adatoms initially adsorbed at oxygen free sites diffuse to O-adsorbed sites that act as centers for the hydrogen desorption.

Carter and her collaborators[25,27] theoretically studied hydrogen desorptions by an *ab initio* derived kinetic Monte Carlo model explicitly treating such hydrogen diffusions. Here, the diffusion is not related to a two-dimensional band-like free state[28] but rather to localized states. They treated the diffusions to lead H atoms to defect sites which catalyze the formation of dihydrides followed by desorption. Consequently, they confirmed that the one-dimensional diffusion along Si dimer rows causes the first-order desorption kinetics. Keeping such a one-dimensional H(D)-atom diffusion in our model so that the first-order desorption kinetics may be ensured, we replace the formation of dihydrides considered in the Carter's model with formation of 2H or 3H configuration followed by desorption. Overcoming diffusion barriers throws H atoms into vibrationally excited states of Si–H bonds. The excess vibrational energies of H atoms may be dissipated to nearby H adatoms via a vibration-vibration energy transfer and to substrate phonons as well. As was theoretically found in a Langmuir-Hinshelwood type associative desorption of vibrationally excited H adatoms,[29] repeated diffusions ($\geqslant$0.1 MHz) to desorption sites would make a steady state nonequilibrium vibrational distribution overpopulated more than a static Boltzmann distribution equilibrated with T_s. Furthermore, according to the diffusion theories[27,30] actual diffusion barriers are lowered by relaxing substrate Si atoms. This means that after H-atom diffusion a fraction of the diffusion barriers is also released to vibrational modes of the substrate Si atoms. In such a circumstance with excessive vibrational energies of H and Si atoms at relevant desorption sites, hydrogen desorption barriers could be thus lowered compared to the case without any H-atom diffusion on H-saturated surfaces or even on patched regions with H-occupied Si-dimer clusters.

Summarizing this section, we illustrate diffusion-promoted interdimer desorption mechanism in Fig. 5. The model picture includes three basic H(D)/Si configurations relevant to the diffusion-promoted 3H and 2H desorptions and nonpromoted 4H one. For high desorption coverage region around 1.0 ML or on patched area filled with doubly occupied Si-dimer clusters,[20] the 4H pathway is not promoted since no dangling bonds are there (Fig. 5, 4H). Desorption rate constant is therefore small because of too high desorption energy barrier [2.84 eV$\pm$0.12 eV (Ref. 15)]. On the other hand, once dangling bonds are created by desorption along the 4H pathway, the promoted 3H pathway is opened when H atoms diffuse from a doubly occupied Si dimer to a neighboring unoccupied Si dimer which was sandwiched by two doubly occupied Si dimers (Fig. 5, 3H). This

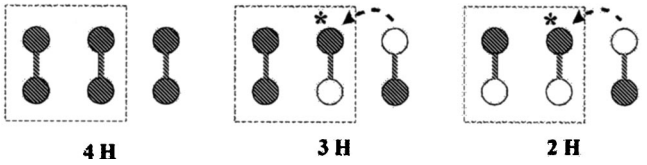

FIG. 5. Three possible configurations for the diffusion-promoted desorption mechanism. Solid circles, H-terminated Si atoms; open circles, non-H-terminated Si atoms. The asterisk stands for the H-terminated Si atoms just after the diffusion indicated by an arrow. 4H, Si dimers are all terminated with H atoms, and thus the desorption cannot be promoted by H-atom diffusion. 3H and 2H, an unoccupied Si dimer is sandwiched by two doubly occupied Si dimers (3H) or one singly and one doubly occupied dimers (2H), respectively. H-atom diffusion from the doubly occupied Si dimer to the dangling bond generates promoted 3H or 2H configuration.

process can be associated with the diffusion of paired hydrogen atoms along the Si dimer rows since the diffusions of two H atoms occur not simultaneously but rather consecutively.[31] Similarly to the 3H situation, as the hydrogen coverages are further decreased the diffusion-promoted 2H pathway will be opened. In this case the desorption reaction occurs as H atoms diffuse from a doubly occupied Si dimer to one of paired Si dangling bonds of which the neighbor is a singly occupied Si dimer (Fig. 5, 2H). As the dangling bond density is further increased at higher T_s the desorption along the 2H pathway will quickly replace the 3H desorption.

V. SUMMARY

We measured the coverage dependent TOF spectra of D_2 molecules thermally desorbed from the D-terminated Si(100) surfaces. The mean translational energies $\langle E_t \rangle$ were found to decrease from 0.40 ± 0.04 eV to 0.20 ± 0.05 eV with increasing coverage. This coverage dependent desorption feature was consistent with the prediction along the interdimer mechanism which consists of three pathways characterized with different adsorption barriers. In the context of detailed balance, the TOF spectra were analyzed with three desorption components along the 2H, 3H, and 4H pathways. As a result, desorptions along the 2H, 3H, and 4H pathways were found to be characterized with mean translational energies of ~ 0.38, ~ 0.21, and ~ 0.12 eV, respectively. On the 1.0 ML D-terminated surface, the desorption kinetics changed from the 4H pathway to the 3H one at the leading edge of the TPD spectrum when less than 0.1 ML D atoms desorbed. As the surface coverage decreased to ~ 0.8 ML the 2H desorption became dominant. In order to explain the apparently smaller contribution of the 4H situation compared with the 2H as well as 3H one, we proposed a desorption mechanism by which the 2H and 3H desorptions are strongly promoted by H(D)-atom diffusion to the dangling bonds relevant to the 2H or 3H configurations, but the 4H desorption is not promoted because of no capability of adatoms to diffuse across the H-terminated area. On the saturated 1.0 ML D/Si(100) surfaces, desorption takes place exclusively along the 4H pathway because of no competing desorption channels. For the reduced surface coverage lower than 0.8 ML, density of the 4H configurations is still large due to clustering of doubly occupied Si dimers.[20] Nevertheless, hydrogen desorption along the 2H (and 3H) pathway prevails the 4H one, indicating desorption rate constant for the 2H pathway must be orders of magnitude larger than that of the 4H pathway. Presumably, the desorption barrier of the 2H situation is substantially decreased compared with the 4H situation due to dynamical effect of the H-atom diffusion on vibrations of H atoms as well as of lattice Si atoms.

ACKNOWLEDGMENT

The authors express their sincere thanks to F. Khanom for her help in drawing the figures.

[1] A. Hodgson, Prog. Surf. Sci. **63**, 1 (2000).
[2] W. Brenig and M. F. Hilf, J. Phys.: Condens. Matter **13**, R61 (2001).
[3] K. W. Kolasinski, W. Nessler, A. de Meijere, and E. Hasselbrink, Phys. Rev. Lett. **72**, 1356 (1994).
[4] M. Dürr, M. B. Raschke, and U. Höfer, J. Chem. Phys. **111**, 10411 (1999).
[5] M. Dürr and U. Höfer, Phys. Rev. Lett. **88**, 076107 (2002).
[6] T. Sagara, T. Kuga, K. Tanaka, T. Shibataka, T. Fujimoto, and A. Namiki, Phys. Rev. Lett. **89**, 086101 (2002).
[7] T. Shibataka, T. Matsuno, H. Tsurumaki, and A. Namiki, Phys. Rev. B **68**, 113307 (2003).
[8] A. Biedermann, E. Knoesel, Z. Hu, and T. F. Heinz, Phys. Rev. Lett. **83**, 1810 (1999).
[9] F. M. Zimmermann and X. Pan, Phys. Rev. Lett. **85**, 618 (2000).
[10] M. Dürr, M. B. Raschke, E. Pehlke, and U. Höfer, Phys. Rev. Lett. **86**, 123 (2001).
[11] M. Dürr, Z. Hu, A. Biedermann, U. Höfer, and T. F. Heinz, Phys. Rev. Lett. **88**, 046104 (2002).
[12] M. Dürr, A. Biedermann, Z. Hu, U. Höfer, and T. F. Heinz, Science **296**, 1838 (2002).
[13] A. Vittadini and A. Selloni, Chem. Phys. Lett. **235**, 334 (1995).
[14] E. Pehlke, Phys. Rev. B **62**, 12932 (2001).
[15] C. Filippi, S. B. Healy, P. Kratzer, E. Pehlke, and M. Scheffler, Phys. Rev. Lett. **89**, 166102 (2002).
[16] W. Brenig, H. J. Kreuzer, and S. H. Payne, Phys. Rev. B **67**, 205419 (2003).
[17] P. Kratzer, R. Russ, and W. Brenig, Surf. Sci. **345**, 125 (1996).
[18] A. J. R. da Silva, M. R. Radeke, and E. A. Carter, Surf. Sci. **381**, L628 (1997).
[19] K. W. Kolasinski, S. F. Shane, and R. N. Zare, J. Chem. Phys. **96**, 3995 (1992).
[20] D. Chen and J. J. Boland, Phys. Rev. Lett. **92**, 096103 (2004).
[21] Z. Hu, A. Biedermann, E. Knoesel, and T. F. Heinz, Phys. Rev. B **68**, 155418 (2003).
[22] M. B. Yilmaz, A. Rajagopal, and M. Zimmermann, Phys. Rev. B **69**, 125413 (2004).
[23] U. Höfer, L. Li, and T. F. Heinz, Phys. Rev. B **45**, 9485 (1992).
[24] J. H. G. Owen, D. R. Bowler, C. M. Goringe, K. Miki, and G. A. D. Briggs, Phys. Rev. B **54**, 14153 (1996).
[25] C. J. Wu, I. V. Ionova, and E. A. Carter, Phys. Rev. B **49**, 13488 (1994).
[26] H. Tsurumaki, K. Iwamura, T. Karato, S. Inanaga, and A. Namiki, Phys. Rev. B **67**, 155316 (2003).
[27] M. R. Radeke and E. A. Carter, Phys. Rev. B **55**, 4649 (1997).
[28] W. Widdra, S. I. Yi, R. Maboudian, G. A. D. Briggs, and W. H. Weinberg, Phys. Rev. Lett. **74**, 2074 (1995).
[29] E. Molinari and M. Tomellinii, Chem. Phys. **270**, 439 (2001).
[30] A. Vittadini, A. Selloni, and M. Casarin, Surf. Sci. **289**, L625 (1993).
[31] D. R. Bowler, J. H. G. Owen, K. Miki, and G. A. D. Briggs, Phys. Rev. B **57**, 8790 (1998).